PCCP

The Atmospheric Importance of Methylamine Additions to Criegee Intermediates

Journal:	*Physical Chemistry Chemical Physics*
Manuscript ID	CP-ART-07-2020-003781.R1
Article Type:	Paper
Date Submitted by the Author:	25-Aug-2020
Complete List of Authors:	Mull, Henry; University of Georgia, Center for Computational Quantum Chemistry Aroeira, Gustavo; University of Georgia, Chemistry Turney, Justin; University of Georgia, Center for Computational Chemistry Schaefer, Henry; University of Georgia, Computational Chemistry

PCCP

ARTICLE TYPE

Cite this: DOI: 00.0000/xxxxxxxxxx

The Atmospheric Importance of Methylamine Additions to Criegee Intermediates†

Henry F. Mull, Gustavo J.R. Aroeira, Justin M. Turney, and Henry F. Schaefer III

Received Date
Accepted Date

DOI: 00.0000/xxxxxxxxxx

Criegee intermediates are important targets for study in atmospheric chemistry because of their capacity to oxidize airborne species. Among these species, ammonia has received critical attention for its presence in polluted agricultural or industrial areas and its role in forming particulate matter and condensation nuclei. Although methylamine has been given less attention than ammonia, both theoretical and experimental studies have demonstrated that the additional methyl substitution on the ammonia derivatives increases the rate constants for some systems. This suggests that the methylamine addition to Criegee intermediates could be more significant to atmospheric processes. In this work, geometries are optimized at the DF-CCSD(T)/ANO1 level for the methylamine addition reactions to the simplest Criegee intermediate and the *anti*- and *syn*-methylated Criegee intermediates. Energies for each stationary point were computed at the CCSD(T)/CBS level with corrections from the CCSDT(Q) method. Rate constants are obtained for each reaction using canonical transition state theory. Although methylamine addition proved to be a more favorable reaction relative to ammonia addition, the significantly lower concentration of atmospheric methylamine limits the prevalence of these reactions, even in the most optimal conditions. It is unlikely that the methylamine addition to Criegee intermediates will contribute significantly to the consumption of Criegee intermediates in the atmosphere.

1 Introduction

Criegee intermediates (CIs) have been the focus of many atmospheric chemistry studies in recent years for the wide range of potential impacts on the atmosphere. They are a class of carbonyl oxides which are formed primarily through the ozonolysis of alkenes in the atmosphere, the mechanism for which was first proposed by Rudolph Criegee in 1949,[1] but they can also be formed through the reaction of peroxy radicals with OH,[2] Br,[3] or Cl radicals.[4] Their highly-reactive and short-lived nature make them difficult targets for experimental studies; however, laboratory techniques to produce CIs have allowed for direct and indirect measurements of CI concentrations and the rate constants of different reaction pathways.[5–14] These experimental studies have been motivated and driven by corresponding theoretical studies, and together they give valuable insight towards the fates of CIs and their effects on the atmosphere.

Part of the importance of CIs in the atmosphere comes from the increased oxidizing capacity of the air as a result of the presence of these species.[15] These reactions are particularly important at times when photochemical reactions are less likely to occur, such as at night or during winter months.[5,16,17] These contributions to the oxidation capacity can occur through a unimolecular transformation, or the intermediates can directly oxidize a variety of airborne species. A majority of the CIs formed will undergo unimolecular decomposition, generating a variety of organic gasses, radicals, and acids,[7,10,18,19] or they can isomerize to form various organic products.[20] Alternatively, the CIs can be collisionally stabilized to form stabilized Criegee intermediates (SCIs) which can survive long enough to further react.[21] A large number of both experimental and theoretical studies have been performed on a variety of atmospheric species including H_2O,[9,13,22–26] CH_4,[27] MeOH,[28] SO_2,[5–7,19,29–31] NO,[30] NO_2,[6,8] NH_3,[11,12,32,33] and $MeNH_2$.[12,34] The majority of SCIs in the atmosphere will be consumed in reactions with water; however, the reactions with other atmospheric species are still possible and are often of greater interest.[30] These sets of reactions can result in the production of particulate matter and cloud condensation nuclei, which are important factors in understanding the air quality and climate of an area.[35–37]

Previous studies of the reaction between SCIs and ammonia or ammonia derivatives show that these reactions have a negligible

Center for Computational Quantum Chemistry, University of Georgia, 140 Cedar Street, Athens, Georgia 30602, USA. Fax: +1 706 542 0406; Tel: +1 706 542 2067; E-mail: ccq@uga.edu

† Electronic Supplementary Information (ESI) available: Optimized geometries, harmonic frequencies, kinetic rates for uncertainty bounds. See DOI: 10.1039/cXCP00000x/

role in the consumption of SCIs. Misiewicz *et al.* investigated the ammonia addition to the simplest SCI and the *anti-* and *syn-*methylated SCIs and determined that this set of reactions would not be able to effectively compete with other similar reactions with more abundant species.[32] This was further confirmed experimentally by Liu *et al.* using OH laser-induced fluorescence[11] and by Chhantyal-Pun *et al.* using cavity ring-down spectroscopy and multiplexed photo-ionization mass spectrometry.[12] However, Kumar and Francisco have recently suggested that increasing the methyl substitution on the ammonia derivative results in a decreased activation barrier.[34] This was also supported experimentally by Chhantyal-Pun *et al.* who found that the reaction between the simplest SCI and methylamine was faster than the corresponding reaction with ammonia.[12] However, Chhantyal-Pun *et al.* only explored the substituent effects of the methylamine, but did not consider the substituent effects of the SCI itself. It has been shown that barrier heights increase and reaction rates decrease with more-substituted SCIs, regardless of the species they are reacting with.[28,32,34] The methylamine addition to simple and methylated SCIs involves both the weakening of the SCI's overall reactivity from increased substitution and the compensation for that loss with the increased reactivity of more-substituted ammonia derivatives. Considering these two effects, the corresponding rates of the reaction could be enhanced to become competitive with the analogous water addition reactions.

Both SCIs and methylamine present their own unique structural challenges. One possible representation of the SCIs is the biradical form with both the terminal oxygen and central carbon having lone electrons. However, Nakajima and Endo experimentally determined the bond lengths and angles of the simplest SCI (CH_2OO) and found that the difference in C-O and O-O bond lengths (1.272 Å and 1.345 Å, respectively) suggested a greater zwitterionic character than biradical character.[14] Additionally, Taatjes *et al.* compared the *syn-* and *anti-* conformers of the methylated SCI and found that the *syn-* conformer was 4 kcal mol^{-1} lower in energy and the interconversion barrier between the two was 40 kcal mol^{-1}, reflecting the zwitterionic character of the SCIs.[13] Methylamine provides a different type of challenge in that both hydrogen atoms are capable of participating in these methylamine addition reactions. This leads to two distinct reaction pathways and starting geometries. In previous work with methylamine, no distinction was made between the two reaction pathways, nor was any justification given for favoring one over the other. Here, the two reaction pathways will be referred to as equatorial and axial. The designations are based on the position of the methylamine methyl group relative to the pseudo five-membered ring formed during the transition state. Equatorial methylamine features the methyl group positioned between the *anti-* and *syn-* positions of the SCI, whereas axial geometries feature the methyl group positioned between the *anti-* position and the double-bond of the SCI (Figure 1). Previously, it seems only the axial addition pathway was considered in computational studies, though whether this is coincidence or by design is unclear.[12,34]

In this research, we examine the methylamine addition to the simplest SCI (CH_2OO) and the *anti-* and *syn-*methylated SCIs

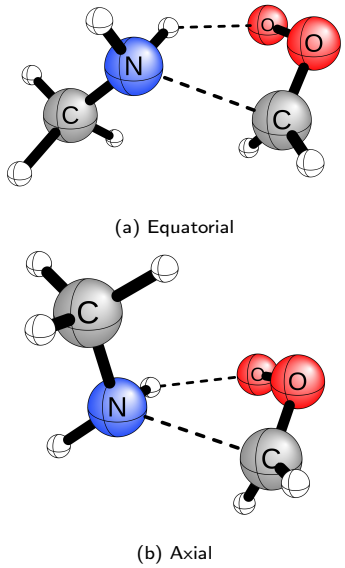

(a) Equatorial

(b) Axial

Fig. 1 The equatorial and axial reaction pathways differ by the orientation of the methylamine methyl group relative to the SCI.

(CH_3CHOO), both the equatorial and axial pathways, using high-level *ab initio* methods. Energies and rate constants are obtained for each of these reactions to understand the combined effect of the substituents on each reactant and the orientation of addition. Comparing these rate constants will determine their importance in the atmosphere relative to each other as well as other atmospheric species.

2 Computational Methods

Each of the geometries investigated was optimized using density-fitted coupled cluster theory with single, double, and perturbative triple excitations [DF-CCSD(T)] with the ANO1 basis set from the atomic natural orbital basis set family,[38] using the ANO1 truncation scheme described by McCaslin and Stanton (C, N, O: [4s 3p 2d 1f]; H: [4s 2p 1s]).[39] Final energies were computed by using the Focal Point Approach (FPA) of Allen and coworkers.[40–42] Restricted Hartree–Fock energies and correlation energies for second-order Møller–Plesset perturbation theory (MP2), CCSD, and CCSD(T) levels of theory were calculated using the Dunning correlation consistent basis sets,[43] cc-pVXZ [X = D, T, Q, 5 for Hartree–Fock energies and X = D, T, Q for MP2, CCSD and CCSD(T)], and then extrapolated to the complete basis set limit (CBS) using the following three–point fitting equation for SCF energies:[44]

$$E_{\mathrm{SCF}} = A + B\exp(-CX)$$

and the following two–point fitting equation for correlation energies:[45]

$$E_{\mathrm{corr}} = A + BX^{-3}$$

Both the energies and the geometries were computed using the frozen core approximation.

A number of additive corrections were obtained for each of the geometries to account for higher-order correlation and approximations made during the energy computations. Zero-point

vibrational energy corrections (Δ_{ZPVE}) were obtained at the DF-CCSD(T) level with the ANO1 basis set for the simple SCI reactions and the ANO0 basis set for the *anti*- and *syn*-SCI reactions. The frozen-core approximation corrective term (Δ_{CORE}) was calculated by taking the difference between the all-electron and frozen core energies at the CCSD(T) level with a weighted core-valence cc-pwCVTZ basis set:[46]

$$\Delta_{CORE} = E_{\text{AE-CCSD(T)}} - E_{\text{FC-CCSD(T)}}$$

The diagonal Born–Oppenheimer correction (Δ_{DBOC}) was calculated at the CCSD level using the ANO0 basis set.[47,48] Corrections for scalar relativistic effects (Δ_{REL}) were calculated using the spin–free X2C-1e method with an X2C-recontracted correlation consistent cc-pCVTZ basis set.[49–54]

$$\Delta_{REL} = E_{\text{AE-CCSD(T)/X2C-1e}} - E_{\text{AE-CCSD(T)}}$$

Our final energies account for higher order correlation using single-point energies at the CCSDT(Q) level and the Dunning cc-pVDZ basis set[43] for the simplest SCI reactions and, due to their size, the Pople 6-31G* basis set for the *anti*- and *syn*-methylated SCI reactions. It has been shown previously by Aroeira *et al.* that for systems involving SCI's the CCSDT(Q) corrections were approximately twice as large as the CCSDTQ corrections,[28]. Their CCSD(T)/CBS, CCSDT(Q)/CBS, and CCSDTQ/CBS computed heats of formation (ΔH_f^{0K}) for the simplest SCI were 27.12, 25.72, and 26.35 kcal mol^{-1}, respectively. While the full CCSDTQ ΔH_f^{0K} matched well with the Active Thermochemical Tables reference value of 26.74 $\pm$ 0.15 kcal mol^{-1}, the CCSD(T) ΔH_f^{0K} was 0.4 kcal mol^{-1} higher and the CCSDT(Q) ΔH_f^{0K} was 1.0 kcal mol^{-1} lower. Recently, Matthews demonstrated the sensitivity of SCIs to higher order corrections by comparing the geometries, energies, and vibrational properties of the simplest SCI using the same methods as above.[55] Again, the CCSDT(Q) results underestimated the CCSDTQ total energy (including Δ_{ZPVE}) by more than 1 kcal mol^{-1}, whereas the CCSD(T) results overestimated the energy by over 2 kcal mol^{-1}. However, these energies were obtained using a structure optimized at their respectively levels of theory, so part of the discrepancy could be due to the difference in geometries. As seen from these examples, we can consider the CCSD(T) and CCSDT(Q) energies as upper and lower bounds to the true energy, where the difference represents the uncertainty range of the computed energy. For the main purposes of this work, the averaged value will be taken as the computed energy, but these bounds will be considered for some qualitative behavior. Thus the final energy discussed here will only include half of the calculated CCSDT(Q) corrective term ($\Delta_{T(Q)}$):

$$E = E_{FPA} + \Delta_{ZPVE} + \Delta_{CORE} + \Delta_{DBOC} + \Delta_{REL} + \frac{\Delta_{T(Q)}}{2}$$

Geometry optimizations and harmonic vibrational frequency calculations were performed with Psi4.[56] Single-point energies for the FPA were calculated using these geometries in the MOLPRO 2010.1 package.[57,58] Corrective terms other than Δ_{ZPVE} were computed using the CFOUR 2.0 quantum chemistry package.[59]

Similarly to previous studies,[28,32] these addition reactions can be represented as:

$$\text{SCI} + \text{NH}_3 \underset{k_{-1}}{\overset{k_1}{\rightleftharpoons}} \text{SCI}\cdots\text{NH}_3 \xrightarrow{k_2} \text{P}$$

where $\text{SCI}\cdots\text{NH}_3$ is a pre-reactive complex and P is the product of the reaction. By employing the Steady State Approximation (SSA),[60] as well as making the assumption of $k_2 << k_{-1}$ which is common for these systems, we can arrive at an expression for our rate constant:

$$\frac{\text{d}[\text{SCI}\cdots\text{NH}_3]}{\text{dt}} = k_1[\text{SCI}][\text{A}] - k_{-1}[\text{SCI}\cdots\text{NH}_3] - k_2[\text{SCI}\cdots\text{NH}_3] = 0$$

$$[\text{SCI}\cdots\text{NH}_3] = \frac{k_1}{k_{-1}+k_2}[\text{SCI}][\text{A}] \approx \frac{k_1}{k_{-1}}[\text{SCI}][\text{A}]$$

$$\frac{\text{d}[\text{P}]}{\text{dt}} = k_2[\text{SCI}\cdots\text{NH}_3] = k_2\frac{k_1}{k_{-1}}[\text{SCI}][\text{A}] = k_2K_c[\text{SCI}][\text{A}]$$

$$k_{tot} = k_2K_c$$

Rate constants can then be calculated using canonical transition state theory,[61,62] with the partition functions (q_A) of each species in the reaction:

$$k_2 = \kappa\frac{k_BT}{h}\frac{q_{\text{TS}}}{q_{\text{SCI}\cdots\text{NH}_3}}\exp\left(\frac{-E_{\text{TS}}}{RT}\right)$$

$$K_c = \frac{q_{\text{SCI}\cdots\text{NH}_3}}{q_{\text{SCI}}q_{\text{NH}_3}}$$

$$k_{tot} = \kappa\frac{k_BT}{h}\frac{q_{\text{TS}}}{q_{\text{SCI}}q_{\text{NH}_3}}\exp\left(\frac{-E_{\text{TS}}}{RT}\right)$$

where κ is the transmission coefficient for an asymmetric Eckhart potential energy barrier:[63]

$$\kappa(T) = \exp\left(\frac{\Delta V_1}{RT}\right)\int_0^\infty \kappa(E)\exp\left(\frac{E}{RT}\right)dE$$

k_B is the Boltzmann constant, R is the universal gas constant, T is temperature, and h is Planck's constant. Canonical transition state theory assumes the high pressure limit which eliminates and pressure dependence in the model. These partition functions are approximated as rigid rotor harmonic oscillators (RRHO), allowing for their total partition functions to be separable into different degrees of freedom:

$$q = q_{trans}q_{rot}q_{vib}q_{elec}$$

3 Results and Discussion

3.1 Geometries

Optimized geometries of the simple, *anti*-, and *syn*- methylamine additions are shown in Figures 2, 3, and 4, respectively. Bond lengths for the pseudo five-membered ring are included and reported in Å. Both the equatorial and axial reaction pathways are shown for comparison. The pre-reactive complexes of the equato-

rial and axial *syn*-SCI additions (Figures 4a and 4b) have a significantly larger C-N distance compared to the simple and *anti*-SCI additions. However, the C-N distances of the corresponding transition states (Figures 4c and 4d) are smaller than those of the simple and *anti*- counterparts. The increased structural change that is required to proceed through the reaction reflects the slower reaction rates of the *syn*-SCI addition reactions, a trend which is expected and has been observed for similar systems.[13,15,32] These geometries also support our choice of SCI representation. Our predictions closely match those of Nakajima and Endo who experimentally determined bond lengths and angles for the simple SCI and concluded that it contained more zwitterion character than biradical character.[14] Furthermore, in each of the reaction pathways, the C-O and O-O bond lengths increase as the reaction proceeds to the product, demonstrating the shift to their normal single bond lengths and further supporting the zwitterion representation.

There exist differences between the equatorial and axial reaction pathways. The largest differences are seen in the pre-reactive complexes for each pair. The positioning of the methylamine methyl group affects how it can approach a given SCI, resulting in a decreased C-N distance and an increased O-H distance for the axial pre-reactive complex compared to the equatorial pre-reactive complex. However, in the transition states for each addition pair, the C-N distance for the equatorial pathway becomes slightly smaller than that of the axial pathway. This is likely due to a smaller amount of steric interference between the methyl groups of the methylamine and the SCI in the equatorial transition states. However, the products of each pair of reactions have bond length differences smaller than 0.1 Å. This is not unexpected as the two products for a given SCI only differ by an inversion and rotation of the amino group.

3.2 Energetics

The FPA tables for all six reactions are presented in Tables 1–6 and good convergence towards the complete basis set limit can be observed in all cases. In all cases, the additive corrections for frozen core, Born–Oppenheimer approximation, and scalar relativistic effects do not exceed 0.11 kcal mol^{-1}, validating the application of these approximations. As was previously noted, the higher-order energy corrections ($\Delta_{T(Q)}$) are taken to be half of the CCSDT(Q) correction to account for the overcorrection of perturbative quadruple excitations relative to full quadruple excitations. Even with this reduction, the higher-order correction can still range from 0.11 to 0.63 kcal mol^{-1}, leading to slight qualitative changes of the potential surface. Our energies are in fairly good agreement with the work done previously by Chhantyal-Pun *et al.*[12] for the axial addition to the simplest SCI using CCSD(T)(F12*)/cc-pVQZ-F12//CCSD(T)(F12*)/cc-pVDZ-F12 energies. However there were some qualitative differences between our work and the work by Kumar and Francisco[34] using CCSD(T)/aug-cc-pVTZ//M06-2X/aug-cc-pVTZ energies, with their barrier heights being lower by at least 0.4 kcal mol^{-1} and up to 1.7 kcal mol^{-1}. If the lower bound of the energies are considered (i.e. without any higher-order correction), the barrier heights are still lower by 0.3 kcal mol^{-1} and up to 1.0 kcal mol^{-1}. Towards the upper bound, the energy differences stemming from higher-order corrections are even further exaggerated and would only increase the difference in barrier height.

The potential energy surfaces for each SCI are shown in Figures 5–7. The equatorial and axial methylamine additions to the simplest SCI have barrier heights of 1.49 kcal mol^{-1} and 1.28 kcal mol^{-1}, respectively. These values only change slightly with the addition of the methyl group at the *anti*- position of the SCI, with barrier heights of 2.13 kcal mol^{-1} and 1.78 kcal mol^{-1}, respectively. This similarity between the two SCIs is expected and has been seen in studies with other systems.[32,34] The barrier heights for the addition to the *syn*-methylated SCIs are 5.49 kcal mol^{-1} for the equatorial addition and 5.03 kcal mol^{-1} for the axial additions. With the SCI methyl group being positioned closer to the oxygen where the hydrogen transfer occurs, significantly more energy is required for the reaction to proceed. This is consistent with the geometries in Figures 4c and 4d, which have much longer bond distances than their simple SCI and *anti*-methylated SCI counterparts. The equatorial addition to the *syn*-methylated SCI has the only non-submerged barrier of this group of reactions; however, it is only 0.45 kcal mol^{-1} and would be unlikely to significantly hinder the reaction from occurring. It is worth noting that if the full $\Delta_{T(Q)}$ correction was included, the axial addition to the *syn*-methylated SCI would no longer be submerged, but the transition state would be above the reactants only by 0.03 kcal mol^{-1} and would not significantly hinder the reaction from occurring.

3.3 Kinetics

Using the final energies and the theoretical frequencies, rate constants for each reaction were calculated and are presented in Table 7. Tunneling does not make significant contributions to these reactions, as the transmission coefficients (κ) only range from 1.044 to 1.089 (Table 8). For the rate constant of the axial methylamine addition to the simplest SCI, our value was in relatively good agreement with a previously calculated value from Chhantyal-Pun *et al.* of 5.6×10^{-12} cm^3 s^{-1} using a micro-canonical master equation,[12] giving us greater confidence in our calculated rate constants for the other five reactions. In the cases of the simple and *anti*-methylated SCIs, the axial addition pathway would be preferred, consistent with our calculated energies and barrier heights. The lowered barrier height and increased reaction rate is likely due to a small stabilizing attractive force between the methyl group of the methylamine and the central oxygen atom. This positions the nitrogen of the methylamine closer to the central carbon of the SCI, so the geometry of the pre-reactive complex and transition state for the axial addition are more similar that those of the equatorial addition, reducing the amount of energy needed for the reaction to proceed. Although a similar case can be made for the methylamine addition to the *syn*-methylated SCI, the small interaction is overshadowed by the additional burden of having to rotate and shift the SCI methyl group.

The effects of methyl substitution can be clearly seen when

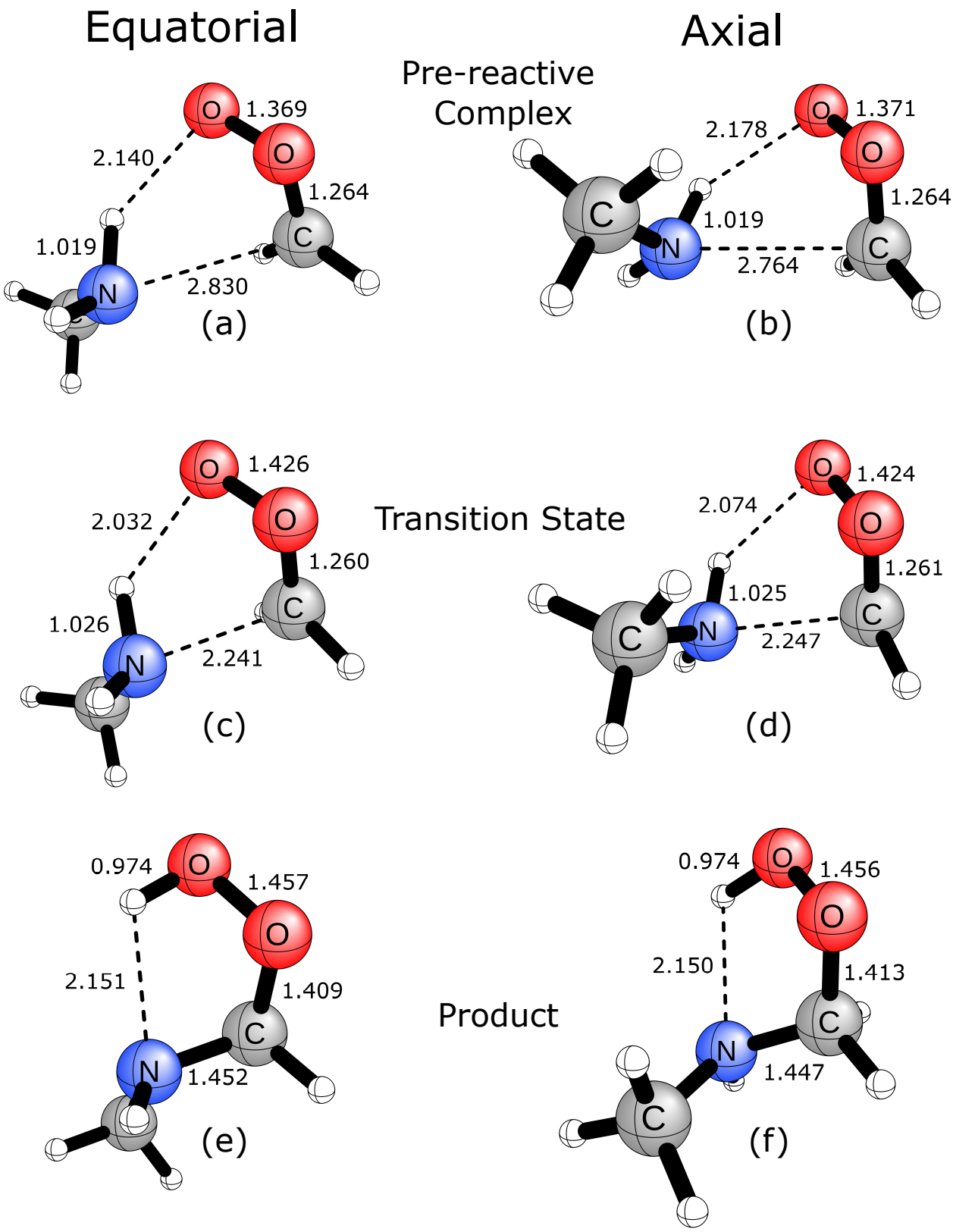

Fig. 2 Optimized CCSD(T)/ANO1 geometries for the pre-reactive complex, transition state, and product of the methylamine addition to the simple Criegee intermediate. Both the equatorial and axial geometries are shown. Distances are given in Å.

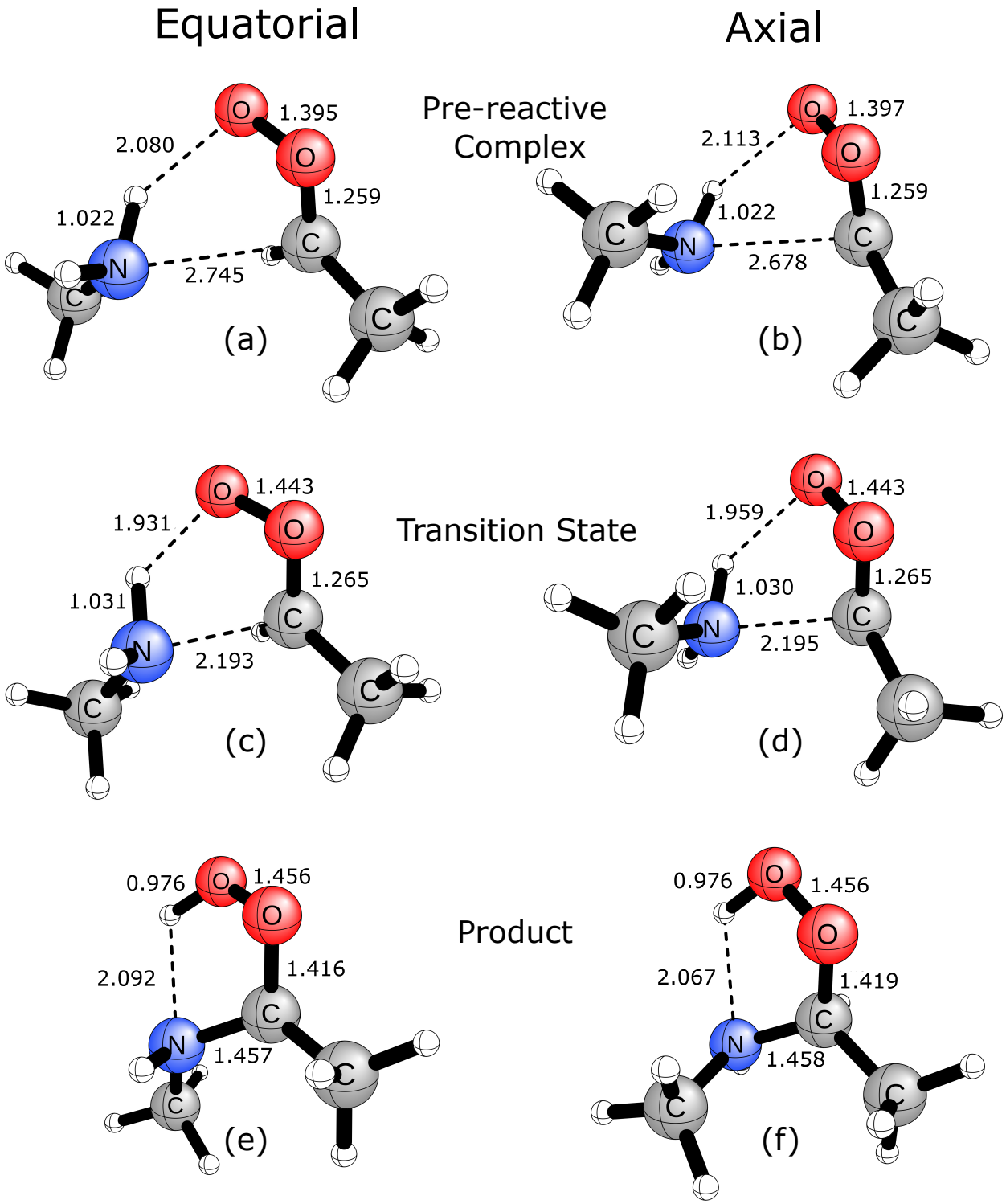

Fig. 3 Optimized CCSD(T)/ANO1 geometries for the pre-reactive complex, transition state, and product of the methylamine addition to the *anti*-Criegee intermediate. Both the equatorial and axial geometries are shown. Distances are given in Å.

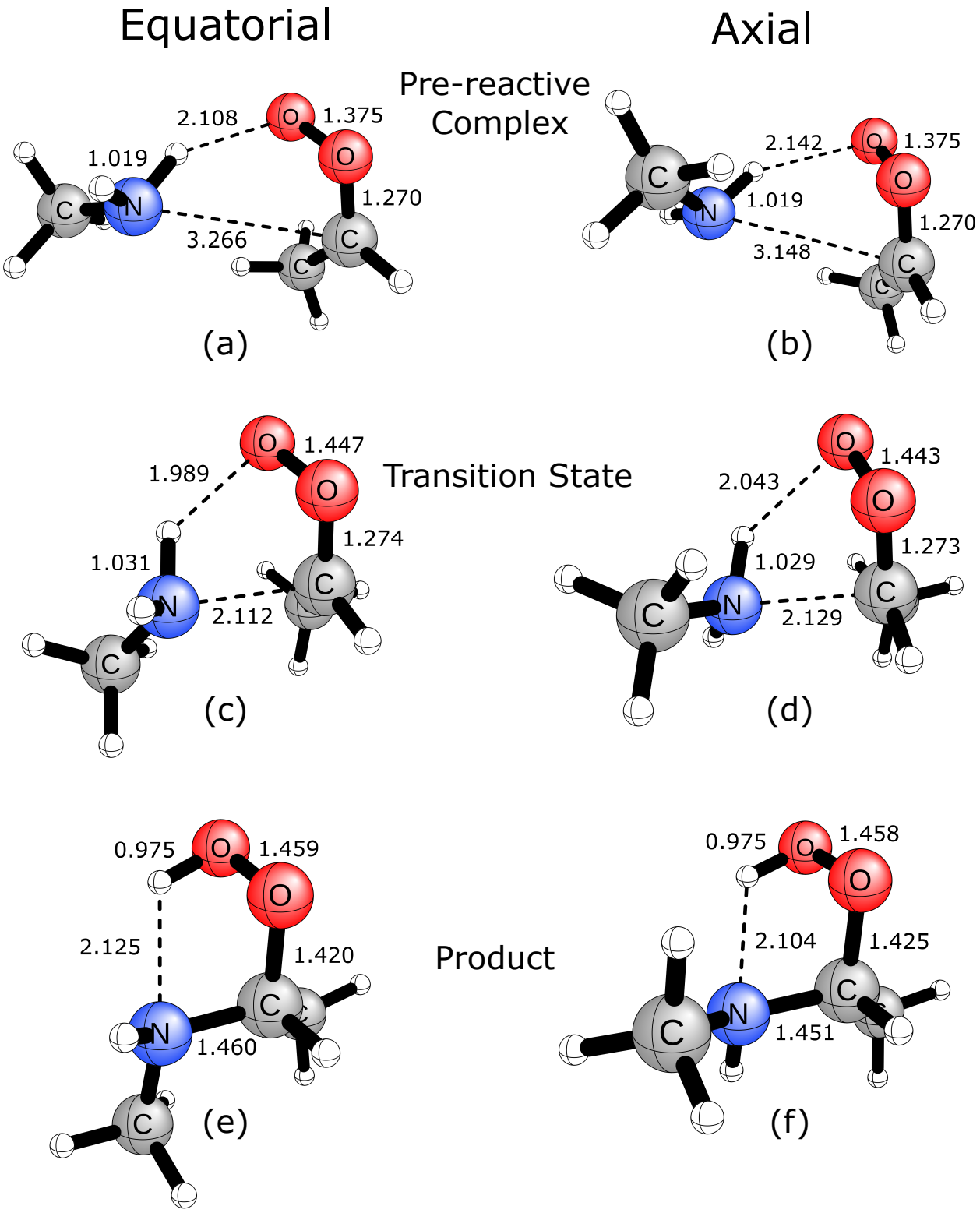

Fig. 4 Optimized CCSD(T)/ANO1 geometries for the pre-reactive complex, transition state, and product of the methylamine addition to the *syn*-Criegee intermediate. Both the equatorial and axial geometries are shown. Distances are given in Å.

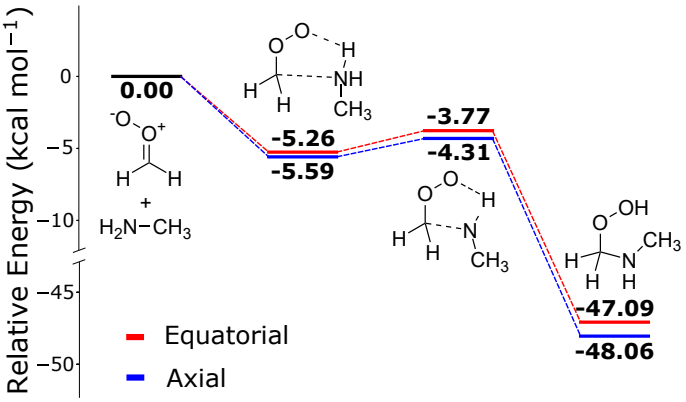

Fig. 5 Enthalpies at 0 K for the methylamine addition to the simplest Criegee intermediate. Energies are computed at CCSD(T)/CBS//DF-CCSD(T)/ANO1 with additive corrections for the zero-point vibrational energy, frozen core approximation, diagonal Born–Oppenheimer correction, scalar relativistic effects, and perturbative quadruple excitations.

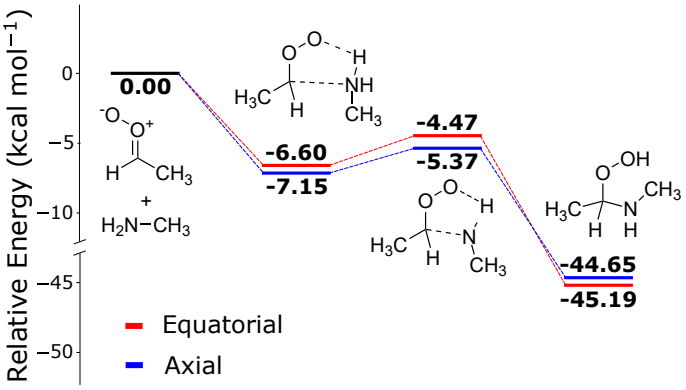

Fig. 6 Enthalpies at 0 K for the methylamine addition to the *anti*-methylated Criegee intermediate. Energies are computed at CCSD(T)/CBS//DF-CCSD(T)/ANO1 with additive corrections for the zero-point vibrational energy, frozen core approximation, diagonal Born–Oppenheimer correction, scalar relativistic effects, and perturbative quadruple excitations.

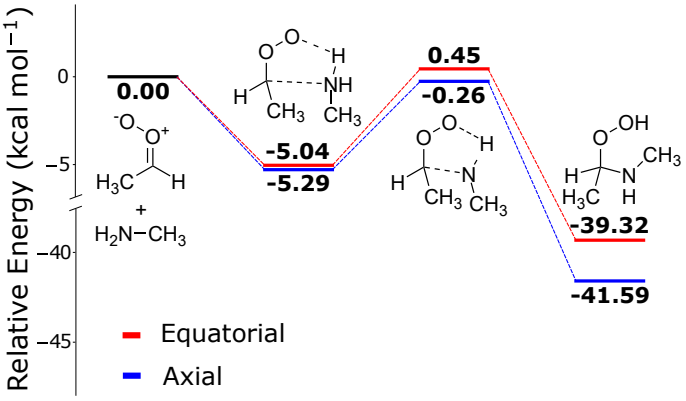

Fig. 7 Enthalpies at 0 K for the methylamine addition to the *syn*-methylated Criegee intermediate. Energies are computed at CCSD(T)/CBS//DF-CCSD(T)/ANO1 with additive corrections for the zero-point vibrational energy, frozen core approximation, diagonal Born–Oppenheimer correction, scalar relativistic effects, and perturbative quadruple excitations.

Table 1 Focal point table for the equatorial addition of methylamine to the simple Criegee intermediate. Energies are given in kcal mol^{-1}. All energies are relative to their isolated reactants (methylamine and the corresponding Criegee intermediate). Final energies in kcal mol^{-1} are presented as $\Delta E = E_{\mathrm{FPA}} + \Delta_{\mathrm{ZPVE}} + \Delta_{\mathrm{CORE}} + \Delta_{\mathrm{DBOC}} + \Delta_{\mathrm{REL}} + \frac{1}{2}\Delta_{\mathrm{T(Q)}}$

Basis Set	ΔE_e RHF	δ MP2	δ CCSD	δ CCSD(T)	ΔE_e Net
Pre-reactive Complex					
cc-pVDZ	−10.87	+2.18	+0.14	+0.96	−7.59
cc-pVTZ	−9.17	+1.04	+0.01	+0.79	−7.33
cc-pVQZ	−8.46	+0.82	−0.16	+0.69	−7.11
cc-pV5Z	−8.08	[+0.74]	[−0.22]	[+0.65]	[−6.92]
CBS	[−7.85]	[+0.65]	[−0.28]	[+0.61]	**[−6.87]**
$\Delta E = -6.87 + 1.43 + 0.00 - 0.01 + 0.01 + 0.19 =$ **−5.26**					
Transition State					
cc-pVDZ	−11.70	+3.51	+1.45	+1.49	−5.25
cc-pVTZ	−9.23	+1.08	+1.05	+1.19	−5.90
cc-pVQZ	−8.44	+0.56	+0.72	+1.00	−6.16
cc-pV5Z	−8.04	[+0.37]	[+0.61]	[+0.93]	[−6.13]
CBS	[−7.80]	[−0.18]	[+0.48]	[+0.85]	**[−6.28]**
$\Delta E = -6.28 + 2.09 + 0.04 - 0.03 + 0.01 + 0.40 =$ **−3.77**					
Product					
cc-pVDZ	−60.07	−1.14	+4.46	+3.87	−52.88
cc-pVTZ	−56.82	−3.23	+3.54	+3.53	−52.98
cc-pVQZ	−55.60	−3.32	+2.95	+3.45	−52.51
cc-pV5Z	−55.01	[−3.35]	[+2.73]	[+3.43]	[−52.20]
CBS	[−54.67]	[−3.38]	[+2.51]	[+3.40]	**[−52.14]**
$\Delta E = -52.14 + 4.44 - 0.08 - 0.04 + 0.11 + 0.63 =$ **−47.09**					

Table 2 Focal point table for the axial addition of methylamine to the simple Criegee intermediates. Energies are given in kcal mol^{-1}. All energies are relative to their isolated reactants (methylamine and the corresponding Criegee intermediate). Final energies in kcal mol^{-1} are presented as $\Delta E = E_{\mathrm{FPA}} + \Delta_{\mathrm{ZPVE}} + \Delta_{\mathrm{CORE}} + \Delta_{\mathrm{DBOC}} + \Delta_{\mathrm{REL}} + \frac{1}{2}\Delta_{\mathrm{T(Q)}}$

Basis Set	ΔE_e RHF	δ MP2	δ CCSD	δ CCSD(T)	ΔE_e Net
Pre-reactive Complex					
cc-pVDZ	−10.86	+1.97	+0.20	+0.91	−7.77
cc-pVTZ	−9.14	+0.64	+0.13	+0.73	−7.64
cc-pVQZ	−8.42	+0.34	−0.01	+0.62	−7.48
cc-pV5Z	−8.05	[+0.23]	[−0.07]	[+0.58]	[−7.31]
CBS	[−7.83]	[+0.11]	[−0.12]	[+0.54]	**[−7.29]**
$\Delta E = -7.29 + 1.53 + 0.00 - 0.01 + 0.01 + 0.19 =$ **−5.59**					
Transition State					
cc-pVDZ	−11.88	+3.28	+1.45	+1.45	−5.70
cc-pVTZ	−9.42	+0.68	+1.11	+1.14	−6.49
cc-pVQZ	−8.61	+0.07	+0.81	+0.93	−6.81
cc-pV5Z	−8.21	[−0.15]	[+0.70]	[+0.85]	[−6.81]
CBS	[−7.98]	[−0.38]	[+0.59]	[+0.77]	**[−6.99]**
$\Delta E = -6.99 + 2.27 + 0.04 - 0.03 + 0.01 + 0.39 =$ **−4.31**					
Product					
cc-pVDZ	−60.71	−1.46	+4.57	+3.86	−53.74
cc-pVTZ	−57.42	−3.65	+3.70	+3.49	−53.87
cc-pVQZ	−56.14	−3.78	+3.11	+3.40	−53.41
cc-pV5Z	−55.56	[−3.83]	[+2.90]	[+3.37]	[−53.11]
CBS	[−55.22]	[−3.88]	[+2.68]	[+3.34]	**[−53.08]**
$\Delta E = -53.08 + 4.42 - 0.09 - 0.04 + 0.11 + 0.63 =$ **−48.06**					

Table 3 Focal point table for the equatorial addition of methylamine to the *anti*-methylated Criegee intermediate. Energies are given in kcal mol^{-1}. All energies are relative to their isolated reactants (methylamine and the corresponding Criegee intermediate). Final energies in kcal mol^{-1} are presented as $\Delta E = E_{\mathrm{FPA}} + \Delta_{\mathrm{ZPVE}} + \Delta_{\mathrm{CORE}} + \Delta_{\mathrm{DBOC}} + \Delta_{\mathrm{REL}} + \frac{1}{2}\Delta_{\mathrm{T(Q)}}$

Basis Set	ΔE_e RHF	δ MP2	δ CCSD	δ CCSD(T)	ΔE_e Net
Pre-reactive Complex					
cc-pVDZ	−11.78	+0.39	+0.88	+0.77	−9.74
cc-pVTZ	−9.53	−0.87	+0.68	+0.52	−9.20
cc-pVQZ	−8.69	−1.01	+0.46	+0.41	−8.83
cc-pV5Z	−8.24	[−1.05]	[+0.38]	[+0.37]	[−8.54]
CBS	[−7.96]	[−1.11]	[+0.30]	[+0.32]	**[−7.12]**
$\Delta E = -8.44 + 1.65 + 0.00 - 0.02 + 0.00 + 0.20 =$					**−6.60**
Transition State					
cc-pVDZ	−8.93	−1.45	+2.63	+0.69	−7.06
cc-pVTZ	−5.90	−3.96	+2.29	+0.25	−7.32
cc-pVQZ	−4.95	−4.31	+1.95	+0.05	−7.25
cc-pV5Z	−4.46	[−4.43]	[+1.83]	[−0.02]	[−7.08]
CBS	[−4.18]	[−4.56]	[+1.70]	[−0.09]	**[−7.12]**
$\Delta E = -7.12 + 2.31 + 0.05 - 0.04 + 0.02 + 0.31 =$					**−4.47**
Product					
cc-pVDZ	−51.80	−8.51	+5.71	+2.60	−52.06
cc-pVTZ	−48.16	−10.47	+5.02	+2.09	−51.52
cc-pVQZ	−46.85	−10.33	+4.50	+2.02	−50.67
cc-pV5Z	−46.19	[−10.29]	[+4.32]	[+2.00]	[−50.17]
CBS	[−45.81]	[−10.24]	[+4.12]	[+1.97]	**[−49.95]**
$\Delta E = -49.95 + 4.33 - 0.05 - 0.04 + 0.10 + 0.42 =$					**−45.19**

Table 4 Focal point table for the axial addition of methylamine to the *anti*-methylated Criegee intermediate. Energies are given in kcal mol^{-1}. All energies are relative to their isolated reactants (methylamine and the corresponding Criegee intermediate). Final energies in kcal mol^{-1} are presented as $\Delta E = E_{\mathrm{FPA}} + \Delta_{\mathrm{ZPVE}} + \Delta_{\mathrm{CORE}} + \Delta_{\mathrm{DBOC}} + \Delta_{\mathrm{REL}} + \frac{1}{2}\Delta_{\mathrm{T(Q)}}$

Basis Set	ΔE_e RHF	δ MP2	δ CCSD	δ CCSD(T)	ΔE_e Net
Pre-reactive Complex					
cc-pVDZ	−11.51	−0.19	+1.04	+0.69	−9.98
cc-pVTZ	−9.23	−1.76	+0.92	+0.41	−9.66
cc-pVQZ	−8.38	−2.01	+0.74	+0.28	−9.38
cc-pV5Z	−7.95	[−2.10]	[+0.67]	[+0.23]	[−9.14]
CBS	[−7.69]	[−2.19]	[+0.61]	[+0.18]	**[−9.09]**
$\Delta E = -9.09 + 1.76 + 0.00 - 0.02 + 0.00 + 0.20 =$					**−7.15**
Transition State					
cc-pVDZ	−9.03	−1.97	+2.73	+0.63	−7.64
cc-pVTZ	−6.00	−4.80	+2.47	+0.16	−8.18
cc-pVQZ	−5.02	−5.25	+2.16	−0.06	−8.17
cc-pV5Z	−4.54	[−5.41]	[+2.06]	[−0.14]	[−8.04]
CBS	[−4.26]	[−5.57]	[+1.94]	[−0.22]	**[−8.12]**
$\Delta E = -8.12 + 2.43 + 0.04 - 0.04 + 0.02 + 0.30 =$					**−5.37**
Product					
cc-pVDZ	−50.73	−9.06	+5.82	+2.58	−51.38
cc-pVTZ	−46.99	−11.13	+5.19	+2.03	−50.90
cc-pVQZ	−45.64	−11.09	+4.69	+1.94	−50.10
cc-pV5Z	−44.99	[−11.07]	[+4.51]	[+1.91]	[−49.64]
CBS	[−44.60]	[−11.05]	[+4.33]	[+1.87]	**[−49.46]**
$\Delta E = -49.46 + 4.39 - 0.07 - 0.05 + 0.11 + 0.42 =$					**−44.65**

Table 5 Focal point table for the equatorial addition of methylamine to the *syn*-methylated Criegee intermediate. Energies are given in kcal mol^{-1}. All energies are relative to their isolated reactants (methylamine and the corresponding Criegee intermediate). Final energies in kcal mol^{-1} are presented as $\Delta E = E_{\mathrm{FPA}} + \Delta_{\mathrm{ZPVE}} + \Delta_{\mathrm{CORE}} + \Delta_{\mathrm{DBOC}} + \Delta_{\mathrm{REL}} + \frac{1}{2}\Delta_{\mathrm{T(Q)}}$

Basis Set	ΔE_e RHF	δ MP2	δ CCSD	δ CCSD(T)	ΔE_e Net
Pre-reactive Complex					
cc-pVDZ	−8.43	−0.59	+0.50	+0.35	−8.18
cc-pVTZ	−6.46	−1.45	+0.41	+0.16	−7.35
cc-pVQZ	−5.68	−1.50	+0.27	+0.09	−6.82
cc-pV5Z	−5.31	[−1.52]	[+0.22]	[+0.06]	[−6.54]
CBS	[−5.09]	[−1.54]	[+0.17]	[+0.04]	**[−6.42]**
$\Delta E = -6.42 + 1.29 - 0.01 - 0.02 + 0.01 + 0.11 =$					**−5.04**
Transition State					
cc-pVDZ	−4.36	−0.87	+2.34	+0.65	−2.24
cc-pVTZ	−1.21	−3.35	+1.95	+0.31	−2.31
cc-pVQZ	−0.28	−3.68	+1.62	+0.13	−2.21
cc-pV5Z	+0.13	[−3.79]	[+1.51]	[+0.06]	[−2.09]
CBS	[+0.36]	[−3.91]	[+1.39]	[+0.00]	**[−2.16]**
$\Delta E = -2.16 + 2.24 + 0.08 - 0.04 + 0.02 + 0.30 =$					**0.45**
Product					
cc-pVDZ	−47.82	−6.36	+4.80	+2.81	−46.59
cc-pVTZ	−44.23	−7.78	+3.99	+2.46	−45.55
cc-pVQZ	−42.96	−7.58	+3.49	+2.43	−44.62
cc-pV5Z	−42.38	[−7.51]	[+3.31]	[+2.42]	[−44.16]
CBS	[−42.06]	[−7.43]	[+3.12]	[+2.41]	**[−43.96]**
$\Delta E = -43.96 + 4.19 - 0.03 - 0.03 + 0.10 + 0.41 =$					**−39.32**

Table 6 Focal point table for the axial addition of methylamine to the *syn*-methylated Criegee intermediate. Energies are given in kcal mol^{-1}. All energies are relative to their isolated reactants (methylamine and the corresponding Criegee intermediate). Final energies in kcal mol^{-1} are presented as $\Delta E = E_{\mathrm{FPA}} + \Delta_{\mathrm{ZPVE}} + \Delta_{\mathrm{CORE}} + \Delta_{\mathrm{DBOC}} + \Delta_{\mathrm{REL}} + \frac{1}{2}\Delta_{\mathrm{T(Q)}}$

Basis Set	ΔE_e RHF	δ MP2	δ CCSD	δ CCSD(T)	ΔE_e Net
Pre-reactive Complex					
cc-pVDZ	−8.54	−0.74	+0.53	+0.31	−8.44
cc-pVTZ	−6.46	−1.69	+0.47	+0.12	−7.55
cc-pVQZ	−5.63	−1.76	+0.34	+0.05	−7.01
cc-pV5Z	−5.25	[−1.79]	[+0.29]	[+0.02]	[−6.73]
CBS	[−5.03]	[−1.82]	[+0.24]	[−0.01]	**[−6.62]**
$\Delta E = -6.62 + 1.24 - 0.01 - 0.02 + 0.01 + 0.11 =$					**−5.29**
Transition State					
cc-pVDZ	−5.08	−0.59	+2.19	+0.67	−2.81
cc-pVTZ	−2.01	−3.17	+1.85	+0.32	−3.01
cc-pVQZ	−1.06	−3.54	+1.54	+0.14	−2.93
cc-pV5Z	−0.65	[−3.68]	[+1.43]	[+0.07]	[−2.83]
CBS	[−0.43]	[−3.82]	[+1.31]	[+0.00]	**[−2.93]**
$\Delta E = -2.93 + 2.32 + 0.07 - 0.04 + 0.02 + 0.29 =$					**−0.26**
Product					
cc-pVDZ	−50.14	−6.18	+4.88	+2.83	−48.62
cc-pVTZ	−46.51	−7.60	+4.09	+2.48	−47.54
cc-pVQZ	−45.19	−7.44	+3.57	+2.45	−46.61
cc-pV5Z	−44.62	[−7.38]	[+3.39]	[+2.43]	[−46.17]
CBS	[−44.30]	[−7.31]	[+3.20]	[+2.42]	**[−45.99]**
$\Delta E = -45.99 + 3.97 - 0.05 - 0.04 + 0.10 + 0.41 =$					**−41.59**

Table 7 Pseudo-first order rate constants for methylamine, ammonia, water, and water dimer addition reactions with Criegee intermediates. Values are calculated at 298 K and under the RRHO approximation. Ammonia is assumed to be at a concentration of 2.5 ppm(v). The mass ratio of methylamine to ammonia is assumed to be 0.026.[64] The water concentration comes from 50% humidity, 298 K and 1 atm. The ratio of water dimer to water is assumed to be 8×10^{-4}.[23] k_{tot} values are presented with units of $cm^3\ s^{-1}$ and k'_{tot} values are presented with units of s^{-1}

	k_{tot}				k'_{tot}		
Species	Simple	*anti*	*syn*	Conc.	Simple	*anti*	*syn*
NH_2CH_3 (Eq)	1.54×10^{-12}	4.50×10^{-12}	2.59×10^{-15}	1.57×10^{-9}	2.42×10^{-21}	7.06×10^{-21}	4.06×10^{-24}
NH_2CH_3 (Ax)	7.34×10^{-12}	1.52×10^{-11}	2.44×10^{-15}		1.15×10^{-20}	2.38×10^{-20}	3.83×10^{-24}
NH_3	5.36×10^{-14} (32)	2.73×10^{-14} (32)	2.70×10^{-18} (32)	1.10×10^{-7}	5.90×10^{-21}	3.00×10^{-21}	2.97×10^{-25}
H_2O	2.40×10^{-16} (24)	1.30×10^{-14} (25)	1.98×10^{-19} (26)	6.31×10^{-4}	1.51×10^{-19}	8.20×10^{-18}	1.25×10^{-22}
$(H_2O)_2$	6.60×10^{-12} (24)	4.40×10^{-13} (25)	2.56×10^{-14} (26)	5.05×10^{-7}	3.33×10^{-18}	2.22×10^{-19}	1.29×10^{-20}

Table 8 Transmission coefficients (κ) for each addition pathway

Pathway	Simple	*anti*	*syn*
Equatorial	1.047	1.044	1.089
Axial	1.043	1.054	1.087

comparing the rate constants of the methylamine additions to the analogous ammonia addition reactions. Rate constants for the preferred axial addition pathway, ammonia addition reactions,[32] water additions, and water dimer additions are compared in Table 7. In all cases, the rate constants for the methylamine addition are significantly greater than those for ammonia and are even comparable to the catalysed water dimer reactions.[25,26]

In order to assess the importance of these addition reactions in the atmosphere, it is helpful to treat these reactions as pseudo-first order reactions. These reactions can all be described by the rate law:

$$\text{rate} = k_{tot}[\text{A}][\text{SCI}]$$

However, if we assume that the concentration of species A remains constant in the atmosphere, which is reasonable considering the small concentration of SCIs in the atmosphere, we can then use the pseudo-first order rate law:

$$\text{rate}' = k'_{tot}[\text{SCI}]$$

which more accurately describes the consumption of SCIs in the atmosphere. Here, an ammonia concentration of 2.5 ppm(v) is assumed based on the work of Jørgenson and Gross[33] with rate constants calculated by Misiewicz *et al.*[32] The mass ratio of methylamine to ammonia is assumed to be 0.026 which is based on high-resolution modeling of atmospheric amines in chemical-industrial regions in China.[64] The water concentration is calculated by assuming 50% humidity with a water dimer to water ratio of 8×10^{-4}.[23] From this, we can see that while the pseudo-first order rate constants for methylamine are greater than those of ammonia by approximately an order of magnitude, they still would not be able to effectively compete with the removal of SCIs by just water alone.

If we were to consider the lower bound of our uncertainty range, where the barrier heights are smaller which result in faster reaction rates, the rate constants for the simple, *anti*-, and *syn*-SCIs are 2.02×10^{-20}, 3.95×10^{-20}, and 6.24×10^{-24} respectively. The methylamine to ammonia ratio used here is on the higher end of the spectrum and is considerably lower in other areas such as agricultural regions with a ratio of 0.0011. Because of this, it is unlikely that a more sophisticated treatment of the kinetics would increase the rate constants significantly to the point that these addition reactions could effectively compete with more common reactions.

4 Conclusions

In this study, we used high-level *ab initio* methods to investigate the addition of methylamine to simple Criegee intermediates and *anti*- and *syn*-methylated Criegee intermediates. Geometries for pre-reactive complexes, transition states, and products were obtained at the DF-CCSD(T)/ANO1 level of theory. Energies for these structures were extrapolated to the CBS limit and included additive corrections for the zero-point vibrational energy, frozen-core approximation, diagonal Born–Oppenheimer correction, scalar relativistic corrections, and higher-order energy corrections. Rate constants for these reactions were calculated using canonical transition state theory and the Steady State Approximation in order to assess the importance of these reactions in the atmosphere.

Of the two reaction pathways that exist for methylamine addition, the axial reaction pathway was found to be preferred. The stationary point geometries were typically lower in energy and the energy barriers were slightly smaller. This was likely due to a small stabilizing interaction between the methyl group of the methylamine and the SCI which is only possible due to the axial orientation of the methylamine. Additionally, it resulted in a more similar pre-reactive complex and transition state than the equatorial counterpart, therefore requiring less energy to proceed with the reaction.

The rate constants for methylamine addition demonstrated how increasing the methyl substitution of the ammonia derivatives positively affects the rate of reaction, increasing by a few orders of magnitude. However, pseudo-first order rate constants which account for the concentration of reactive species in the atmosphere allow for a more direct comparison of the various atmospheric species. These pseudo-first order rate constants, while still larger than those of ammonia, are still significantly less than those for water or the water dimer, and would likely fall short of most other atmospheric species. Even in the most optimal conditions, it is unlikely for methylamine to significantly affect the

concentration of SCIs in the atmosphere.

Conflicts of interest

There are no conflicts to declare.

Acknowledgements

We acknowledge support from the US Department of Energy (DOE), Office of Science, Office of Basic Energy Sciences (BES), Computational and Theoretical Chemistry (CTC) Program under Contract No. DE-SC0018412.

References

1 V. R. Criegee and G. Wenner, *Liebigs Ann. Chem.*, 1949, **564**, 9–15.

2 E. Assaf, L. Sheps, L. Whalley, D. Heard, A. Tomas, C. Schoemaecker and C. Fittschen, *Environ. Sci. Technol.*, 2017, **51**, 2170–2177.

3 D. E. Shallcross, K. E. Leather, A. Bacak, P. Xiao, E. P. Lee, M. Ng, D. K. Mok, J. M. Dyke, R. Hossaini, M. P. Chipperfield, M. A. H. Khan and C. J. Percival, *J. Phys. Chem.*, 2015, **119**, 4618–4632.

4 T. Jungkamp, A. Kukui and R. Schindler, *Ber. Bunsenges. Phys. Chem.*, 1995, **99**, 1057–1066.

5 N. Sarnela, T. Jokinen, J. Duplissy, C. Yan, T. Nieminen, M. Ehn, S. Schobesberger, M. Heinritzi, S. Ehrhart, K. Lehtipalo, J. Tröstl, M. Simon, A. Kürten, M. Leiminger, M. J. Lawler, M. P. Rissanen, F. Bianchi, A. P. Praplan, J. Hakala, A. Amorim, M. Gonin, A. Hansel, J. Kirkby, J. Dommen, J. Curtius, J. N. Smith, T. Petäjä, D. R. Worsnop, M. K. ad Neil M. Donahue and M. Sipilä, *Atmos. Chem. Phys.*, 2018, **18**, 2363–2380.

6 O. Welz, J. D. Savee, D. L. Osborn, S. S. Vasu, C. J. Percival, D. E. Shallcross and C. A. Taatjes, *Science*, 2012, **335**, 204–207.

7 M. C. Smith, W. Chao, K. Takahashi, K. A. Boering and J. J.-M. Lin, *J. Phys. Chem.*, 2016, **120**, 4789–4798.

8 B. Ouyang, M. W. McLeod, R. L. Jones and W. J. Bloss, *Phys. Chem. Chem. Phys.*, 2013, **15**, 17070–17075.

9 A. S. Hasson, M. Y. Chung, K. T. Kuwata, A. D. Converse, D. Krohn and S. E. Paulson, *J. Phys. Chem.*, 2003, **107**, 6176–6182.

10 A. Novelli, L. Vereecken, J. Lelieveld and H. Harder, *Phys. Chem. Chem. Phys.*, 2014, **16**, 19941–19951.

11 Y. Liu, C. Yin, M. C. Smith, S. Liu, M. Chen, X. Zhou, C. Xiao, D. Dai, J. J.-M. Lin, K. Takahashi, W. Dong and X. Yang, *Phys. Chem. Chem. Phys.*, 2018, **20**, 29669–29676.

12 R. Chhantyal-Pun, R. J. Shannon, D. P. Tew, R. L. Carvan, M. Duchi, C. Wong, A. Ingham, C. Feldman, M. R. McGillen, M. A. H. Khan, I. O. Antonov, B. Rotavera, K. Ramasesha, D. L. Osborn, C. A. Taatjes, C. J. Percival, D. E. Shallcross and A. J. Orr-Ewing, *Phys. Chem. Chem. Phys.*, 2019, **21**, 14042–14052.

13 C. A. Taatjes, O. Welz, A. J. Eskola, J. D. Savee, A. M. Scheer, D. E. Shallcross, B. Rotavera, E. P. Lee, J. M. Dyke, D. K. Mok, D. L. Osborn and C. J. Percival, *Science*, 2013, **340**, 177–180.

14 M. Nakajima and Y. Endo, *J. Chem. Phys.*, 2013, **139**, 101103.

15 M. Khan, C. Percial, R. Caravan, C. Taatjes and D. Shallcross, *Environ. Sci.: Processes Impacts*, 2018, **20**, 437–453.

16 Y. Elshorbany, R. Kurtenbach, P. Wiesen, E. Lissi, M. Rubio, G. Villena, E. Gramsh, A. Rickard, M. Pilling and J. Kleffman, *Atmos. Chem. Phys.*, 2009, **9**, 2257–2273.

17 R. Harrison, J. Yin, R. Tilling, X. Cai, P. Seakins, J. Hopkins, D. Lansley, A. Lewis, M. Hunter, D. Heard, L. Carpenter, D. Creasey, J. Lee, M. J. Pilling, N. Carslaw, K. Emmerson, A. Redington, R. Derwent, D. Ryall, G. Mills and S. Penkett, *Sci. Total Environ.*, 2006, **360**, 5–25.

18 O. Horie and G. Moortgat, *Atmos. Environ.*, 1991, **25**, 1881–1896.

19 D. M. Meidan, J. S. Holloway, P. M. Edwards, W. Dubé, A. M. Middlebrook, J. Liao, A. Welti, M. Graus, C. Warneke, T. B. Ryerson, I. B. Pollack, S. S. Brown and Y. Rudich, *ACS Earth Space Chem.*, 2019, **3**, 748–759.

20 J. Kalinowski, M. Räsänen, P. Heinonen, I. Kilpeläinen and R. B. Gerber, *Angew. Chem. Int. Ed.*, 2014, **53**, 265–268.

21 T. L. Nguyen, H. Lee, D. A. Matthews and M. C. McCarthy, *J. Phys. Chem.*, 2015, **119**, 5524–5533.

22 A. B. Ryzhkov and P. A. Ariya, *Chem. Phys. Lett.*, 2006, **419**, 479–485.

23 B. Long, J. L. Bao and D. G. Truhlar, *J. Am. Chem. Soc.*, 2016, **138**, 14409–14422.

24 L. Sheps, B. Rotavera, A. J. Eskola, D. L. Osborn, C. A. Taatjes, K. Au, D. E. Shallcross, M. A. H. Khan and C. J. Percival, *Phys. Chem. Chem. Phys.*, 2017, **19**, 21970–21979.

25 L. C. Lin, H. T. Chang, C. H. Chang, W. Chao, M. C. Smith, C. H. Chang, J. Jr-Min Lin and K. Takahashi, *Physical Chemistry Chemical Physics*, 2016, **18**, 4557–4568.

26 L. C. Lin, W. Chao, C. H. Chang, K. Takahashi and J. J. M. Lin, *Physical Chemistry Chemical Physics*, 2016, **18**, 28189–28197.

27 K. Xu, W. Wang, W. Wei, W. Feng, Q. Sun and P. li, *J. Phys. Chem.*, 2017, **121**, 7236–7245.

28 G. J. Aroeira, A. S. Abbot, S. N. Elliot, J. M. Turney and H. F. Schaefer, *Phys. Chem. Chem. Phys.*, 2019, **21**, 17760–17771.

29 J. Li, Q. Ying, B. Yi and P. Yang, *Atmos. Environ.*, 2013, **79**, 442–447.

30 L. Vereecken, H. Harder and A. Novelli, *Phys. Chem. Chem. Phys.*, 2012, **14**, 14682–14695.

31 C. J. Percival, O. Welz, A. J. Eskola, J. D. S. nd David L. Osborn, D. O. Topping, D. Lowe, S. R. Utembe, A. Bacak, G. McFiggans, M. C. Cooke, P. Xiao, A. T. Archibald, M. E. Jenkin, R. G. Derwent, I. Riipinen, D. W. Molk, E. P. Lee, J. M. Dyke, C. A. Taatjes and D. E. Shallcross, *Faraday Discuss.*, 2013, **165**, 45–73.

32 J. P. Misiewicz, S. N. Elliott, K. B. Moore and H. F. Schaefer, *Phys. Chem. Chem. Phys.*, 2018, **20**, 7479–7491.

33 S. Jørgensen and A. Gross, *J. Phys. Chem.*, 2009, **113**, 10284–10290.

34 M. Kumar and J. S. Francisco, *Chem. Sci.*, 2019, **10**, 743–751.

35 F. Raes and R. V. Dingenen, *J. Geophys. Res. - Atmos*, 1992, **97**, 12901–12912.

36 R. J. Charlson, D. S. Covert, T. V. Larson and A. P. Waggoner, *Atmos. Environ.*, 1978, **12**, 39–53.

37 C. R. Ruehl, J. F. Davies and K. R. Wilson, *Science*, 2016, **351**, 1447–1450.

38 J. Almlöf and P. R. Taylor, *J. Chem. Phys.*, 1987, **86**, 4070–4077.

39 L. McCaslin and J. Stanton, *Mol. Phys.*, 2013, **111**, 1492–1496.

40 L. N. Appelhans, D. Zuccaccia, A. Kovacevic, A. R. Chianese, J. R. Miecznikowski, A. Macchioni, E. Clot, O. Eisenstein and R. H. Crabtree, *J. Am. Chem. Soc.*, 2005, **127**, 16299–16311.

41 A. G. Császár, W. D. Allen and H. F. Schaefer, *J. Chem. Phys.*, 1998, **108**, 9751–9764.

42 M. S. Schuurman, S. R. Muir, W. D. Allen and H. F. Schaefer, *J. Chem. Phys.*, 2004, **120**, 11586–11599.

43 T. H. Dunning, *J. Chem. Phys.*, 1989, **90**, 1007–1023.

44 D. Feller, *J. Chem. Phys.*, 1993, **98**, 7059–7071.

45 T. Helgaker, W. Klopper, H. Kock and J. Noga, *J. Chem. Phys.*, 1997, **106**, 9639–9646.

46 K. A. Peterson and T. H. Dunning, *J. Chem. Phys.*, 2002, **117**, 10548–10560.

47 H. Sellers and P. Pulay, *Chem. Phys. Lett.*, 1984, **103**, 463–465.

48 N. Handy, Y. Yamaguchi and H. F. Schaefer, *J. Chem. Phys.*, 1986, **84**, 4481–4484.

49 K. Dyall, *J. Chem. Phys.*, 1997, **106**, 9618–9626.

50 W. Kutzelnigg and W. Liu, *J. Chem. Phys.*, 2005, **123**, 241102.

51 W. Liu and D. Peng, *J. Chem. Phys.*, 2006, **125**, 044102.

52 M. Iliaš and T. Saue, *J. Chem. Phys.*, 2007, **126**, 064102.

53 J. Sikkema, L. Visscher, T. Saue and M. Iliăs, *J. Chem. Phys.*, 2009, **131**, 124116.

54 W. Liu and D. Peng, *J. Chem. Phys.*, 2009, **131**, 031104.

55 D. Matthews, *J. Chem. Theory Comput.*, in press.

56 R. M. Parrish, L. A. Burns, D. G. Smith, A. C. Simmonett, A. E. DePrince, E. G. Hohenstein, U. Bozkaya, A. Y. Sokolov, R. D. Remigio, R. M. Richard, J. F. Gonthier, A. M. James, H. R. McAlexander, A. Kumar, M. Saitow, X. Wang, B. P. Pritchard, P. Verma, H. F. Schaefer, K. Patowski, R. A. King, E. F. Valeev, F. A. Evangelista, J. M. Turney, T. D. Crawford and C. D. Sherrill, *J. Chem. Theory Comput.*, 2017, **13**, 3185–3197.

57 H.-J. Werner, P. J. Knowles, G. Knizia, F. R. Manby and M. Schütz, *WIREs Comput Mol Sci*, 2012, **2**, 242–253.

58 H.-J. Werner, P. J. Knowles, G. Knizia, F. R. Manby, M. Schütz, P. Celani, W. Györffy, D. Kats, T. Korona, R. Lindh, A. Mitrushenkov, G. Rauhut, K. R. Shamasundar, T. B. Adler, R. D. Amos, S. J. Bennie, A. Bernhardsson, A. Berning, D. L. Cooper, M. J. O. Deegan, A. J. Dobbyn, F. Eckert, E. Goll, C. Hampel, A. Hesselmann, G. Hetzer, T. Hrenar, G. Jansen, C. Köppl, S. J. R. Lee, Y. Liu, A. W. Lloyd, Q. Ma, R. A. Mata, A. J. May, S. J. McNicholas, W. Meyer, T. F. Miller III, M. E. Mura, A. Nicklass, D. P. O'Neill, P. Palmieri, D. Peng, K. Pflüger, R. Pitzer, M. Reiher, T. Shiozaki, H. Stoll, A. J. Stone, R. Tarroni, T. Thorsteinsson, M. Wang and M. Welborn, *MOLPRO, version 2019.2, a package of ab initio programs*, 2019, see https://www.molpro.net.

59 J. F. Stanton, J. Gauss, L. Cheng, M. E. Harding, D. A. Matthews and P. G. Szalay, *CFOUR, Coupled-Cluster techniques for Computational Chemistry, a quantum-chemical program package*, With contributions from A.A. Auer, R.J. Bartlett, U. Benedikt, C. Berger, D.E. Bernholdt, Y.J. Bomble, O. Christiansen, F. Engel, R. Faber, M. Heckert, O. Heun, M. Hilgenberg, C. Huber, T.-C. Jagau, D. Jonsson, J. Jusélius, T. Kirsch, K. Klein, W.J. Lauderdale, F. Lipparini, T. Metzroth, L.A. Mück, D.P. O'Neill, D.R. Price, E. Prochnow, C. Puzzarini, K. Ruud, F. Schiffmann, W. Schwalbach, C. Simmons, S. Stopkowicz, A. Tajti, J. Vázquez, F. Wang, J.D. Watts and the integral packages MOLECULE (J. Almlöf and P.R. Taylor), PROPS (P.R. Taylor), ABACUS (T. Helgaker, H.J. Aa. Jensen, P. Jørgensen, and J. Olsen), and ECP routines by A. V. Mitin and C. van Wüllen. For the current version, see http://www.cfour.de.

60 K. J. Laidler, *Pure Appl. Chem.*, 1996, **68**, 149–192.

61 K. J. Laidler and M. C. King, *J. Phys. Chem.*, 1983, **87**, 2657–2664.

62 D. G. Truhlar, B. C. Garrett and S. J. Klippenstein, *J. Phys. Chem.*, 1996, **100**, 12771–12800.

63 H. Johnston and J. Heicklen, *J. Phys. Chem.*, 1962, **66**, 532–533.

64 J. Mao, F. Yu, Y. Zhang, J. An, L. Wang, J. Zheng, L. Yao, G. Luo, W. Ma, Q. Yu, C. Huang, L. Li and L. Chen, *Atmos. Chem. Phys.*, 2018, **18**, 7933–7950.

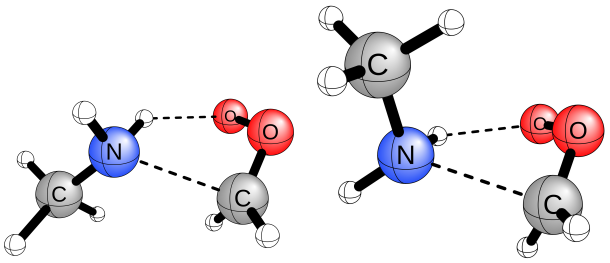

The methylamine addition to Criegee intermediates is investigated using high level *ab initio* methods.